

**FABRICATION AND CHARACTERIZATION OF AGAR BASED
ANTHROPOMORPHIC ULTRASOUND BREAST PHANTOM**

by

SEYEDEH PARISA FOROOZANDEHASL

Thesis submitted in fulfillment of the requirements
for the degree of
Master of Science

March 2012

**FABRIKASI DAN PENCIRIAN FANTOM PAYUDARA
ANTROPOMORIFK BERASASKAN AGAR**

oleh

SEYEDEH PARISA FOROOZANDEHASL

Tesis yang diserahkan untuk
memenuhi keperluan bagi
Ijazah Sarjana Sains

Mac 2012

ACKNOWLEDGEMENTS

First and foremost, all praise and thanks is to Allah S.W.T. the Lord of the universe that has given me the strength and opportunity to complete this research.

I am heartily thankful to my supervisor Prof. Dr. Mohamad Suhaimi Bin Jaafar who was abundantly helpful and offered valuable assistance, support and guidance.

I would like to thank to Medical Physics laboratory Assistants Mr. Yahya Ibrahim and Mr. Azmi Bin Abdullah. I would like to show my gratitude to Physics and Chemistry laboratories of Universiti Pendidikan Sultan Idris. I would also like to express my sincere thanks to Mr. Noor Mazlan Bin Mohamed, Physics laboratory Assistant of Universiti Pendidikan Sultan Idris and Mohammad Tajuddin B Asm Nagoor Gany. I would like to express my appreciation to Prof. Rosly jaafar for his great – by all means – guidance and assistance.

I owe my deepest gratitude to my beloved parents, for their faith in me, their understanding and endless love and allowing me to be as ambitious as I wanted. It was under their watchful eye that I gained so much drive and an ability to tackle challenges head on. This thesis would not have been possible without all sacrifices that my lovely parents have done to enable me to complete my study.

Lastly, I would like to dedicate this thesis to someone who tried all his life to guide me toward the success and made available his support in a number of ways during all my life. That is my late father Seyed Hossein Foroozandehasl.

TABLE OF CONTENTS

Title Page		i
Acknowledgment		iii
Table of Contents		iv
List of Tables		ix
List of Figures		x
List of Abbreviations		xvii
List of Symbols		xviii
Abstrak		xix
Abstract		xxi
CHAPTER 1	INTRODUCTION	
1.1	Background	1
1.2	Statement of Problems	3
1.3	Objectives	4
1.4	Scope of Research	4
1.5	Outline of the Thesis	4
CHAPTER 2	LITERATURE REVIEW	
2.1	Ultrasound	6
2.1.1	Characteristic of ultrasound wave	7
2.1.1.1	Frequency of ultrasound wave	7
2.1.1.2	Velocity of ultrasound wave	8
2.1.1.3	Wavelength of ultrasound wave	10
2.1.1.4	Amplitude of ultrasound wave	12
2.1.2	Intensity of ultrasound wave	12

2.1.3	Acoustical impedance	13
2.1.4	Interactions of ultrasound pulse with matter	14
2.1.4.1	Reflection of ultrasound pulse	14
2.1.4.2	Refraction of ultrasound pulse	16
2.1.4.3	Attenuation of ultrasound pulse	17
2.1.5	Acoustic properties measurement	20
2.1.5.1	Sound speed measurement	20
2.1.5.2	Attenuation measurement	21
2.1.6	Artifacts in ultrasound images	21
2.1.6.1	Reverberation artifact in ultrasound images	22
2.1.6.2	Mirror image artifact in ultrasound images	23
2.1.6.3	Side lobe artifacts in ultrasound images	24
2.1.6.4	Acoustic shadowing artifact in ultrasound images	25
2.2	Phantom	26
2.2.1	Hydro gel based phantom	27
2.2.2	Agar based phantom	27
2.3	Anatomy of the breast	28
2.3.1	Lobules and ducts	29
2.3.2	Stromata	30
2.3.3	Lymph nodes and lymph ducts	31
2.4	Breast phantom	31

CHAPTER 3

METHODOLOGY

3.1	Fabrication of breast phantom	34
3.1.1	Fabrication of TM glandular tissue	35

3.1.2	Fabrication of TM fat	36
3.1.3	Fabrication of TM cyst	37
3.1.4	Assembly of the breast phantom	37
3.2	The applied method to characterize the fabricated breast phantom	40
3.2.1	Density measurement	40
3.2.2	Acoustic properties measurement	41
3.2.2.1	Sound speed measurement	46
3.2.2.2	Attenuation measurement	46
3.3	Weight composition variation to characterize the fabricated breast phantom	48
3.3.1	Variation in weight composition of agar	48
3.3.2	Variation in weight composition of alcohol	49
3.3.3	Variation in weight composition of anise oil	51
3.4	Temperature variation to characterize the fabricated breast phantom	52
3.5	Acquisition of ultrasound image	54
3.5.1	Ultrasound needle visualization	55

CHAPTER 4

RESULT ON CHARACTERIZATION OF FABRICATED PHANTOM

4.1	Density of phantom samples	57
4.2	Weight composition variation of agar	66
4.2.1	Sound speed with varying weight composition of agar	60
4.2.2	Attenuation coefficient with varying weight composition of agar	61

4.2.3	Acoustic impedance with varying weight composition of agar	63
4.2.4	Reflection coefficient with varying weight composition of agar	64
4.2.5	Bulk modulus with varying weight composition of agar	65
4.3	Weight composition variation of alcohol	66
4.3.1	Sound Speed with varying weight composition of alcohol	66
4.3.2	Attenuation coefficient with varying weight composition of alcohol	67
4.3.3	Acoustic impedance with varying weight composition of alcohol	69
4.3.4	Reflection coefficient with varying weight composition of alcohol	70
4.3.5	Bulk modulus with varying weight composition of alcohol	71
4.4	Weight composition variation of anise oil	72
4.4.1	Sound speed with varying weight compositions of anise oil	72
4.4.2	Attenuation coefficient with varying weight compositions of anise oil	73
4.4.3	Acoustic impedance with varying weight compositions of anise oil	75
4.4.4	Reflection coefficient with varying weight compositions of anise oil	76
4.4.5	Bulk modulus with varying weight compositions of anise oil	77
4.5	Temperature variation	78
4.5.1	Sound speed with temperature variation	78
4.5.2	Attenuation coefficient with temperature variation	80
4.5.3	Acoustic impedance with temperature variation	82
4.5.4	Reflection coefficient with temperature variation	83

	4.5.5	Bulk modulus with temperature variation	84
4.6		Frequency variation	85
	4.6.1	Sound speed with frequency variation	85
	4.6.2	Attenuation coefficient with frequency variation	88
4.7		Properties of TM glandular tissue over time	93
	4.7.1	Sound speed over time	93
	4.7.2	Attenuation coefficient over time	93
	4.7.3	Acoustic impedance over time	95
	4.7.4	Reflection coefficient over time	95
	4.7.5	Bulk modulus over time	95
4.8		Durability test of fabricated breast phantom	97
CHAPTER 5		RESULT OF ULTRASOND IMAGING ON FABRICATED BREAST PHANTOM	
	5.1	TM fat and TM cyst visualization	99
	5.2	Needle visualization	104
CHAPTER 6		CONCLUSION	
	6.1	Conclusions	107
	6.2	Recommendations	134
REFERENCES			110

LIST OF TABLES

Table 2.1	Approximate velocity of sound in different part of human body	9
Table 2.2	Acoustic impedance of human tissues	13
Table 3.1	Weight composition of used materials in TM glandular tissue for the fabrication of phantom samples with different percentage of agar.	49
Table 3.2	Weight composition of used materials in TM glandular tissue for the fabrication of phantom samples with different percentage of alcohol	50
Table 3.3	Weight composition of used materials in TM fat for the fabrication of phantom samples with different percentage of anise oil	51
Table 4.1	Density of phantom samples with different percentage of agar	58
Table 4.2	Density of phantom samples with different percentage of 2-isopropyl alcohol	58
Table 4.3	Density of phantom samples with different percentage of anise oil	59

LIST OF FIGURES

Figure 2.1	Ultrasound wave is transmitted to the body by the transducer and is reflected from the surface and produce the echo which form the ultrasound image	7
Figure 2.2	The length characteristics of an ultrasound pulse	11
Figure 2.3	Dependency of ultrasound pulse length on wavelength and frequency	11
Figure 2.4	Reflected ultrasound beam from interface between two tissues. θ_i is the angle of incidence, θ_r is the angle of reflection and θ_t is the angle of transmission	16
Figure 2.5	The passing ultrasound wave at the interface between two matters and produce refraction and bending. θ_1 is the angle of incidence and θ_2 is the angle of refraction	16
Figure 2.6	The effect of absorption on ultrasound pulse amplitude in relation to distance or depth in the body	18
Figure 2.7	Ultrasound attenuation coefficient as a function of frequency for various tissue samples	19
Figure 2.8	Reverberation artifacts (white arrows) can be seen during needle (yellow arrows) advancement in the infraclavicular region using a curved transducer	22
Figure 2.9	Longitudinal US image obtained at the level of the right hepatic lobe shows an echogenic lesion in the right hepatic lobe (cursors) and a duplicated echogenic lesion (arrow) equidistant from the diaphragm overlying the expected location of lung parenchyma	23
Figure 2.10	Side lobe artifact is seen overlying the fetal head (arrows). The artifactual nature of these echoes can be confirmed by noting that these echoes are not confined to the head but extend beyond its confines	24
Figure 2.11	An acoustic shadow artifact (hypoechoic region = bone shadow) deep to a hyperechoic bone outline (arrows) is the result of beam attenuation when the beam encounters bone with a high attenuation coefficient	25
Figure 2.12	The position of female breast and its different parts	29
Figure 2.13	Lobules and duct in the breast	30

Figure 2.14	Stromata fat and ligaments in the breast	30
Figure 2.15	Breast profile includes of; ducts (A), lobules (B), dilated section of duct to hold milk (C), nipple (D), fat (E), pectoralis major muscle (F) and chest wall/rib cage (G). Enlargement picture shows; normal duct cells (A), basement membrane (B), and lumen (center of duct) (C)	31
Figure 3.1	The sagittal view of fabricated anthropomorphic breast phantom	34
Figure 3.2	Agar solution was heated by hot plate to reach 90°C for fabricating TM glandular tissue of anthropomorphic breast phantom	35
Figure 3.3	Fabricated TM fat of anthropomorphic breast phantom	36
Figure 3.4	Prepared TM cyst of anthropomorphic breast phantom	37
Figure 3.5	TM glandular tissue with fabricated TM fat and TM cyst	38
Figure 3.6	Fabricated anthropomorphic breast phantom in supine position	38
Figure 3.7	(a) The fabricated breast phantom with its housing. (b) The Fabricated anthropomorphic breast phantom while it is removed from its housing	39
Figure 3.8	Schematic illustration of the set up that was used in the experiment for the acquisition of signals measuring the acoustic properties. Transducer T sends an ultrasound pulse that travels through the phantom and is received by transducer R, and it was monitored by digital oscilloscope	41
Figure 3.9	The set up that was used in the experiment to measure the time shift and amplitude of ultrasound pulse	42
Figure 3.10	Inserted PMMA block in the test cell which was filled with distilled water to calibrate the equipment	43
Figure 3.11	Time shift of ultrasound pulse through the PMMA block, recorded at frequency of 5 MHz	43
Figure 3.12	Amplitude of ultrasound pulse through the PMMA block, recorded at frequency of 5 MHz	44
Figure 3.13	Transit time of ultrasound pulse through the distilled water, recorded at frequency of 5 MHz	45
Figure 3.14	Amplitude of ultrasound pulse through the distilled water, recorded at frequency of 5 MHz	45

Figure 3.15	Aluminum mould which was used to cut the phantom samples	46
Figure 3.16	Phantom sample in rectangular shape with 26 mm thickness	46
Figure 3.17	The time shift of ultrasound pulse through the phantom sample, recorded at frequency of 5 MHz	47
Figure 3.18	Amplitude of ultrasound pulse through the phantom sample, recorded at frequency of 5 MHz	47
Figure 3.19	The phantom samples with different percentage of agar	48
Figure 3.20	The fabricated phantom samples with different percentage of alcohol	50
Figure 3.21	Fabricated phantom samples with different percentage of anise oil	51
Figure 3.22	Water bath used to increase the temperature over the room temperature	53
Figure 3.23	Digital thermometer used to monitor the temperature of phantom sample	53
Figure 3.24	Ultrasound imaging device used to acquire ultrasound image from fabricated breast phantom	54
Figure 3.25	The biopsy needle that was used to approach the TM cyst and TM fat	56
Figure 4.1	The effect of weight composition variation of agar on the sound speed of phantom samples at different frequencies	62
Figure 4.2	The effect of weight composition variation of agar on the attenuation coefficient of phantom samples at different frequencies	62
Figure 4.3	The effect of weight composition variation of agar on acoustic impedance of phantom samples at different frequencies	63
Figure 4.4	The effect of weight composition variation of agar on the reflection coefficient of phantom samples at different frequencies	64
Figure 4.5	The effect of weight composition variation of agar on bulk modulus of phantom samples at different frequencies	65

Figure 4.6	The effect of weight composition variation of alcohol on the sound speed of phantom samples at different frequencies	68
Figure 4.7	The effect of weight composition variation of alcohol on the attenuation coefficient of phantom samples at different frequencies	68
Figure 4.8	The effect of weight composition variation of alcohol on the acoustic impedance of phantom samples at different frequencies	69
Figure 4.9	The effect of weight composition variation of alcohol on the reflection coefficient of phantom samples at different frequencies	70
Figure 4.10	The effect of weight composition variation of alcohol on bulk modulus of phantom samples at different frequencies	71
Figure 4.11	The effect of anise oil concentration variation on the sound speed of phantom samples at different frequencies	74
Figure 4.12	The effect of anise oil concentration variation on the attenuation coefficient of phantom samples at different frequencies	74
Figure 4.13	The effect of anise oil concentration variation on acoustic impedance of fabricated phantom samples at different frequencies	75
Figure 4.14	The effect of the anise oil concentration on the reflection coefficient of phantom samples at different frequencies	76
Figure 4.15	The effect of anise oil concentration variation on bulk modulus of phantom samples at different frequencies	77
Figure 4.16	The effect of temperature variation on the sound speed of phantom sample	79
Figure 4.17	The regression analysis on sound speed against temperature for the phantom sample at a frequency of 5 MHz	79
Figure 4.18	The effect of temperature variation on the attenuation coefficient of phantom sample	81
Figure 4.19	Regression analysis on attenuation coefficient against temperature for phantom sample at frequency of 5 MHz	81
Figure 4.20	The effect of temperature variation on the acoustic impedance of fabricated phantom samples	82

Figure 4.21	The effect of the temperature variation on reflection coefficient of phantom sample	83
Figure 4.22	The effect of temperature variation on bulk modulus of phantom sample	84
Figure 4.23	The effect of the frequency variation on the sound speed for different percentages of agar	86
Figure 4.24	The effect of frequency variation on the sound speed for different percentages of alcohol	87
Figure 4.25	The effect of frequency variation on the sound speed of phantom samples with different percentages of oil	87
Figure 4.26	The effect of frequency variation on the attenuation coefficient for different percentages of agar	88
Figure 4.27	The effect of frequency variation on the attenuation coefficient of phantom samples with different percentages of alcohol	89
Figure 4.28	The effect of frequency variation on the attenuation coefficient of phantom samples with different percentages of anise oil	89
Figure 4.29	Regression analysis on attenuation coefficient against frequency (in a range of 2.25 to 10 MHz) for phantom samples with different percentage of agar	90
Figure 4.30	Regression analysis on attenuation coefficient against frequency (in a range of 2.25 to 10 MHz) for phantom samples with different percentage of alcohol	91
Figure 4.31	Regression analysis on attenuation coefficient against frequency (in a range of 2.25 to 10 MHz) for phantom samples with different percentage of anise oil	92
Figure 4.32	Sound speed of phantom sample over time. The measurements were done from 9:00 am to 9:00 am on the next day. Note that the single point at the right side of the figure shows the measured value at 9:00 am on the next day	94
Figure 4.33	Attenuation coefficient of phantom sample over time. The measurements were done from 9:00 am to 9:00 am on the next day. Note that the single point at the right side of the figure shows the measured value at 9:00 am on the next day	94
Figure 4.34	Acoustic impedance of phantom sample over time. The measurements were done from 9:00 am to 9:00 am on the	96

	next day. Note that the single point at the right side of the figure shows the measured value at 9:00 am on the next day	
Figure 4.35	Reflection coefficient of phantom sample over time. The measurements were done from 9:00 am to 9:00 am on the next day. Note that the single point at the right side of the figure shows the measured value at 9:00 am on the next day	96
Figure 4.36	Bulk modulus of phantom sample over time. The measurements were done from 9:00 am to 9:00 am on the next day. Note that the single point at the right side of the figure shows the measured value at 9:00 am on the next day	97
Figure 4.37	Shrunken of the fabricated breast phantom and fungus appear on fabricated breast phantom due to the open air exposure after 9 days	98
Figure 4.38	More fungus appeared on fabricated breast phantom due to the open air exposure after 12 days	98
Figure 5.1	Ultrasound convex probe was placed on the top surface of the fabricated breast phantom to obtain ultrasound image	100
Figure 5.2	The ultrasound image shows the fabricated TM fat and TM cyst when the convex probe is placed on the top surface of the fabricated breast phantom. The blue arrow indicates the TM cyst and the red arrow indicates the TM fat	100
Figure 5.3	Ultrasound convex probe was placed at right side of the fabricated breast phantom to obtain ultrasound image	101
Figure 5.4	The ultrasound image shows the fabricated TM fat and TM cyst when the convex probe is placed at left side of the fabricated breast phantom. The blue arrow indicates the TM cyst and the red arrow indicates the TM fat	101
Figure 5.5	Ultrasound convex probe was placed on the bottom surface of the fabricated breast phantom to obtain ultrasound image	102
Figure 5.6	The ultrasound image shows the fabricated TM fat and TM cyst when the convex probe is placed on the bottom surface of the fabricated breast phantom. The blue arrow indicates the TM cyst and the red arrow indicates the TM fat	102
Figure 5.7	Ultrasound convex probe was placed at left side of the fabricated breast phantom to obtain ultrasound image	103
Figure 5.8	The ultrasound image shows the fabricated TM fat and TM cyst when the convex probe is placed on the left side of the fabricated breast phantom. The blue arrow indicates the TM cyst and the red arrow indicates the TM fat	103

Figure 5.9	Biopsy needle inserted through the fabricated breast phantom. The needle can be visualized from the acquired ultrasound image	104
Figure 5.10	The ultrasound image of fabricated breast phantom shows the needle through the fabricated cyst	105
Figure 5.11	The ultrasound image of fabricated breast phantom shows the needle through the fabricated fat	105
Figure 5.12	Sonogram of fabricated breast phantom shows the needle passing through both the fabricated cyst and fat	106

LIST OF ABBREVIATIONS

B-mode	Brightness mode
CT	Computed Tomography
CW	Continuous Wave
IEC	International Electrotechnical Commission
MRI	Magnetic Resonance Imaging
PAA	Polyacrylamide gel
PVA	Polyvinyl Alcohol gel
PW	Pulsed Wave
QA	Quality Assurance
TGC	Time Gain Compensation
TM	Tissue Mimicking
TMM	Tissue Mimicking Material
US	Ultrasound

LIST OF SYMBOLS

α	Attenuation coefficient
β	Compressibility
λ	Wavelength of wave
ρ	Density
A	Amplitude of transmitted wave
A_0	Reference amplitude
$^{\circ}\text{C}$	Degree Celsius
cm	Centimeter
dB	Decibel
dB cm⁻¹	Decibel per centimeter
dB cm⁻¹ MHz⁻¹	Decibel per centimeter per Megahertz
E	Energy of wave
f	Frequency
g	Gram
g cm⁻³	Gram per centimeter cube
Hz	Hertz
I	Transmitted intensity
I_0	Reference intensity
K	Bulk modulus
m s⁻¹	Meter per second
MHz	Megahertz
R	Reflection coefficient
T	Period of wave
Z	Acoustic impedance

Fabrikasi dan Pencirian Fantom Payudara Antropomorfik Berasaskan Agar

ABSTRAK

Suatu fantom payudara antropomorfik berasaskan agar, termasuklah TM tisu kelenjar tak adipos, TM lemak dan sista TM telah difabrikasikan. Pencirian telah dilakukan terhadap fantom yang difabrikasi dan kebergantungannya kepada komposisi berat, suhu, frekuensi dan masa dikaji. Kelajuan bunyi dan pekali pengecilan telah diukur dengan menggunakan teknik penggantian penghantaran dengan tiga transduser jalur lebar yang berpusat di 2.25, 5 dan 10MHz. Impedans akustik, pekali pantulan dan modulus pukal fantom yang difabrikasi juga dibuat penilaian.

Kelajuan bunyi, di dalam fantom payudara berasaskan agar yang difabrikasi, sebagai fungsi peningkatan komposisi berat agar telah meningkat pada seluruh julat 1487 ms^{-1} hingga 1540 ms^{-1} , pekali pengecilan telah meningkat dari 0.66 hingga 0.90 $\text{dB cm}^{-1} \text{ MHz}^{-1}$ untuk 2.25 MHz, 0.66 hingga 1.71 $\text{dB cm}^{-1} \text{ MHz}^{-1}$ untuk 5 MHz dan 1.10 hingga 2.46 $\text{dB cm}^{-1} \text{ MHz}^{-1}$ untuk 10 MHz. Impedans akustik, pekali pantulan dan modulus pukal juga meningkat dengan peningkatan kepekatan agar. Kelajuan bunyi dalam fantom terfabrikasi meningkat dengan peningkatan komposisi berat alkohol, merentasi julat 1483 hingga 1510 ms^{-1} , pekali pengecilan meningkat dari 0.10 kepada 0.23 $\text{dB cm}^{-1} \text{ MHz}^{-1}$ untuk 2.25 MHz, 0.34 hingga 0.59 $\text{dB cm}^{-1} \text{ MHz}^{-1}$ untuk 5 MHz dan 0.85 hingga 0.92 $\text{dB cm}^{-1} \text{ MHz}^{-1}$ untuk 10 MHz. Impedans akustik, pekali pantulan dan modulus pukal juga meningkat dengan peningkatan peratusan alkohol. Peningkatan komposisi berat minyak anise, menyebabkan berkurang kelajuan bunyi dalam julat 1501 ms^{-1} hingga 1517 ms^{-1} , pekali pengecilan meningkat

dari 0.15 hingga 1.02 dB cm⁻¹ MHz⁻¹ untuk 2.25 MHz, 0.47 hingga 1.89 dBcm⁻¹MHz⁻¹ untuk 5 MHz dan 0.87 hingga 2.76 dB cm⁻¹ MHz⁻¹ untuk 10 MHz. Impedans akustik, pekali pantulan dan modulus pukal menurun dengan peningkatan peratusan minyak anise. Kelajuan bunyi menunjukkan tren kenaikan dengan suhu merentasi julat 1466 hingga 1602 ms⁻¹, pekali pengecilan didapati menurun dengan peningkatan suhu dengan kadar 0.003 dB cm⁻¹ MHz⁻¹ °C⁻¹. Impedans akustik, pekali pantulan dan modulus pukal meningkat dengan suhu. Sebagai fungsi frekuensi, kelajuan bunyi, impedans akustik, pekali pantulan dan modulus pukal semuanya kekal hampir malar dengan peningkatan frekuensi tetapi pekali pengecilan meningkat dengan ketara dengan frekuensi yang semakin meningkat.

Fantom payudara yang difabrikasi adalah sesuai untuk latihan pengimejan ultrasound dan prosedur biopsi, memandangkan ciri-cirinya yang hampir dengan badan manusia. Tambahan pula, fantom yang difabrikasi ini adalah tidak mahal, tahan lama dan terbiodegradasikan.

Fabrication and Characterization of Agar Based Anthropomorphic Ultrasound Breast Phantom

ABSTRACT

An anthropomorphic agar based breast phantom including tissue mimicking (TM) non adipose glandular tissue, TM fat and TM cyst was been fabricated. The fabricated phantom was characterized and the weight composition, temperature, frequency and time dependencies of the phantom were investigated. The sound speed and attenuation coefficient were measured by using the transmission substitution technique with three broadband transducers with 2.25, 5 and 10 MHz frequencies. Acoustic impedance, reflection coefficient and bulk modulus of fabricated breast phantom were also assessed.

The sound speed, in fabricated agar based breast phantom, as a function of increasing weight composition of agar was increased across the range from 1487 ms^{-1} to 1540 ms^{-1} . Attenuation coefficient was increased from 0.66 to 0.90 $\text{dB cm}^{-1} \text{ MHz}^{-1}$ for 2.25 MHz, 0.66 to 1.71 $\text{dB cm}^{-1} \text{ MHz}^{-1}$ for 5 MHz and 1.10 to 2.46 $\text{dB cm}^{-1} \text{ MHz}^{-1}$ for 10 MHz. Acoustic impedance, reflection coefficient and bulk modulus also increased with increasing concentration of agar. The sound speed of fabricated breast phantom increased by increasing the weight composition of alcohol, across the range from 1483 to 1510 ms^{-1} . Attenuation coefficient increased from 0.10 to 0.23 $\text{dB cm}^{-1} \text{ MHz}^{-1}$ for 2.25 MHz, 0.34 to 0.59 $\text{dB cm}^{-1} \text{ MHz}^{-1}$ for 5 MHz and 0.85 to 0.92 $\text{dB cm}^{-1} \text{ MHz}^{-1}$ for 10 MHz. Acoustic impedance, reflection coefficient and bulk modulus also increased with the increasing percentage of alcohol. Increasing the weight composition of anise oil caused the reduction in the sound speed in the range of 1517 ms^{-1} to 1501 ms^{-1} . Attenuation coefficient increased from 0.15 to 1.02 $\text{dB cm}^{-1} \text{ MHz}^{-1}$ for 2.25 MHz, 0.47 to 1.89 $\text{dB cm}^{-1} \text{ MHz}^{-1}$ for 5 MHz

and 0.87 to 2.76 dB cm⁻¹ MHz⁻¹ for 10 MHz. Acoustic impedance, reflection coefficient and bulk modulus decreased with the increasing percentage of anise oil. The sound speed showed an increment trend with temperature across the range of 1466 to 1602 ms⁻¹. Attenuation coefficient was found to decrease by increasing the temperature by a rate of 0.003 dB cm⁻¹ MHz⁻¹ °C⁻¹. Acoustic impedance, reflection coefficient and bulk modulus increased with temperature. As a function of frequency, sound speed, acoustic impedance, reflection coefficient and bulk modulus all remained almost constant with increasing frequency but the attenuation coefficient increased significantly by increasing frequency.

The fabricated breast phantom is suitable for ultrasound imaging and biopsy procedure training, as its characteristics are approximate to that of the human body. Furthermore, this fabricated phantom was inexpensive, durable and biodegradable.

CHAPTER ONE

INTRODUCTION

1.1 Background

Ultrasonography is the application of ultrasound to produce an image from a small part of the inner organs like prostate, thyroid and breast. Ultrasound wave is transmitted to the human body by a transducer that converts electrical energy into mechanical energy and the echoes were digitally processed to form an ultrasound image. Ultrasonography is relatively inexpensive, non-ionizing, non-invasive and able to produce images in real time. This imaging technique is applied in several medical fields such as gynecology, obstetric, thyroid, prostate and female breast study.

The ultrasonography on breast presents valuable information about tissue structure of the breast. Ultrasonography can distinguish the malignant or benign solid tumor, cysts and the palpable breast lesions (Athanasidou *et al.*, 2010). The ultrasonography and physical tests enable the physicians to identify more than 90% of malignant lesions over 1cm. According to the free ionized radiation of the ultrasonography, it is a safe examination on the human body and may be performed several times on the human organs in all ages (Griffiths, 1978). Furthermore, one of the applications of ultrasonography is in the awareness of breast screening among women for an early preventive response against breast cancer.

Moreover, ultrasonography is applied for breast biopsy where the organs tissue of interest is removed by using a needle for laboratory examinations. The biopsy has to be done properly and guided by using ultrasonography. During the biopsy procedure, the movement of the needle approaching the solid mass can be seen from an ultrasound image acquired.

For the past few decades, there is a growing rate of using ultrasound in medical imaging as well as ultrasound phantoms for different parts of the human body are increasingly developed. Phantoms are used to mimic different parts of human organ such as breast, thyroid, liver and foetus. The ultrasound phantoms for each type of human organs are widely used as a realistic and life-like model for practical ultrasound applications.

Ultrasound phantoms are structures that contain one or more materials that simulate the tissue in its interaction with ultrasound. The phantom can be a homogeneous slab of tissue mimicking material or contain some embedded target with known size, shape and position.

Tissue-mimicking phantoms operate as an essential instrument for checking the performance in ultrasonography systems and medical physics training aims. Therefore, the optimal phantom materials represent the physical characteristics similar to human body organs (Zell *et al.*, 2007). The phantoms can be used for different purposes such as training, education, quality assurance, as well as research and development of ultrasonographic equipment.

1.2 Statement of problems

For clinical testing of an ultrasonography system performance, the tissue mimicking material (TMM) for phantom must have the same range of sound speeds, attenuation coefficients and backscatter, as the organ they aim to mimic. At present, commercially available phantoms are not fitted for this purpose, due to the acoustic properties of the TMMs used in their production. The TMMs are homogeneous and have a uniform speed of sound of 1540 ms^{-1} , hence, the artifacts introduced in a clinical situation would not exist neither the performed tests could not be compared to clinically reported findings. In general, the ideals mentioned for phantoms are not satisfactorily achievable with commercially available phantoms (Browne *et al.*, 2004).

In addition, commercially available phantoms are all similar in design, consisting in general of nylon filaments and tissue mimicking cylindrical objects (representing anechoic and contrast structures) embedded in a homogeneous tissue mimicking background material (Browne *et al.*, 2004; Browne *et al.*, 2005).

Similarly, there is a simple commercial breast phantom at the Medical Physics laboratory, Universiti Sains Malaysia that is not included of any target and also is not much fitting for using in ultrasonography imaging and biopsy training. Thus, it is crucial to fabricate a phantom included of simulated fat and cyst that can be suitable for biopsy training and needle visualization.

1.3 Objectives of Research

The objectives of this research are as follows:

1. To design and fabricate an anthropomorphic breast phantom including tissue mimicking (TM) glandular tissue, TM fat and TM cyst.
2. To characterize weight compositions, frequency, temperature and time variations of properties of fabricated breast phantom.
3. To acquire ultrasound images on fabricated anthropomorphic breast phantom in order to visualize the TM fat, TM cyst and biopsy needle insertion.

1.4 Scope of Research

The scope of research is fabricating the agar based breast phantom that can be utilized in ultrasound imaging and biopsy training. The study focuses on measuring the acoustical properties of fabricated breast phantom and also visualization of the simulated fat and cyst in ultrasonography procedure. The breast phantom, to be fabricated, will match human breast characteristic such as the sound speed and attenuation coefficient. The materials to be used are consumer products, recyclable material and non toxic.

1.5 Outline of the thesis

This thesis presents a description on a fabricated breast phantom to be used for training and biopsy ultrasonography. In chapter 1, the background for the ultrasound breast phantom, statement of problems, objectives and scope of the thesis were

described. Chapter 2 reviews the theory of ultrasound and a brief literature review of the previous studies and fabrication of ultrasound phantoms. Chapter 3 presents the methodology of the research, including the materials and methods for fabricating the breast phantom, the set-up of experiment and laboratorial measurements. Chapter 4 is devoted to results and discussions on characterization of the properties of the fabricated breast phantom and evaluation of the weight compositions, frequency, temperature and time dependencies of properties of the fabricated breast phantom. Chapter 5 presents results and discussions of ultrasound imaging on the fabricated breast phantom and interpretation of ultrasound images. Finally, chapter 6 covers the conclusions of the study and the recommendations for further research.

CHAPTER TWO

THEORY AND LITERATURE REVIEW

2.1 Ultrasound

Ultrasound is a sound wave with frequency greater than 20 kHz. In ultrasound diagnostic, frequencies in the range of 2 MHz to 20 MHz are used. Ultrasound imaging is a type of medical imaging, which uses high frequency to detect and perform image processing of inner organs or blood flow.

Ultrasound transducer which is in contact with patient's body via water based gel, convert electrical pulse to ultrasound pulse or in another word the electrical pulse causes the transducer crystal to vibrate. Ultrasound wave is propagated through the human body and is partly reflected by the tissue boundaries and detected by the transducer which is called the ultrasound echo.

Echoes are produced by surfaces or boundaries between two different types of tissues and give informations about the location, dimension and orientation of the organ which was scanned. Echoes that are received by the transducer converted back into electrical pulses and form an ultrasound image (Hendee and Ritenour, 2002; Sprawls, 1993). The basic ultrasound imaging process is illustrated in Figure 2.1.

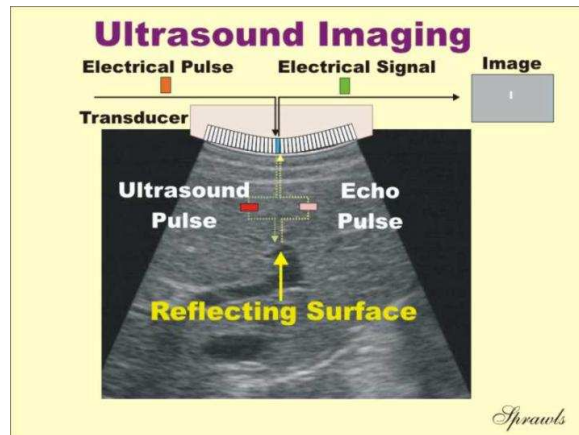


Figure 2.1. Ultrasound wave is transmitted to the body by the transducer and is reflected from the surface and produce the echo which form the ultrasound image (Sprawls, 1993).

2.1.1 Characteristic of ultrasound wave

Ultrasound waves have a number of acoustical specifications that are important to consider for adjusting the scanning procedure for specific diagnostic purposes. Ultrasound pulses are characterized by their frequency, velocity, wavelength, and amplitude.

2.1.1.1 Frequency of ultrasound wave

Frequency is the number of fluctuations of a particular particle in per unit of time. In SI unit, the unit for the wave frequency is hertz (Hz). Frequency is stated cycles per unit of time as given by equation 2.1.

$$Frequency (Hz) = \frac{Cycle}{Time (second)} \quad (2.1)$$

Selecting the ultrasound wave frequency is important in order to generate an appropriate balance between scan specifications and penetration depth. Generally, ultrasound waves with higher frequency create an image with better resolution, but these pulses cannot penetrate through the deeper organs (Hendee and Ritenour, 2002; Sprawls, 1993).

2.1.1.2 Velocity of ultrasound wave

Wave velocity introduces as speed of sound wave when it propagates through a media and refers to the distance that is traveled by a sound wave per unit of time. Wave velocity implies both speed and direction. In general, sound velocity is determined by the characteristics of the medium, and it does not have dependency on the characteristic of the sound wave. The velocity of the ultrasound pulse in a liquid type medium like human tissues is obtained by using equation 2.2.

$$wave\ velocity = \sqrt{\frac{K}{\rho}} \quad (2.2)$$

where ρ is the density of media and K is a parameter which is called bulk modulus and is related to the elastic properties or stiffness of the medium. Bulk modulus is defined as a ratio of the change in pressure to the rate of volume variation due to the change in pressure. Bulk modulus (K) can also be expressed in term of density variations as given by equation 2.3. (Kothandaraman and Rudramoorthy, 2007; Bhargava, 2002).

$$K = -dp \left(\frac{dv}{v} \right) = dp \left(\frac{d\rho}{\rho} \right) \quad (2.3)$$

where dp is the change in the pressure causing a change in volume dV when the original volume was V . It is known that $(dV/V) = - (d\rho/\rho)$

The bulk modulus in a fluid can be calculated according to the Newton-Laplace formula as given in equation 2.4. The SI unit of the bulk modulus is N/m^2 or Pa.

$$K = \rho v^2 \tag{2.4}$$

where, ρ determines the density and v the speed of sound.

For instance, the velocities of sound wave through various human organs are presented in Table 2.1.

Table 2.1. Approximate velocity of sound wave in different parts of the human body (Hendee and Ritenour, 2002).

Medium	Sound Velocity (ms^{-1})
Fat	1475
Soft tissue	1540
brain	1560
Kidney	1560
Spleen	1570
Blood	1570
Liver	1570
Muscle	1580
Lenses of eyes	1620
Skull bone	3360

Approximately, all ultrasonography systems are set up to determine positions of the structures by using an assumed velocity about 1540 ms^{-1} . It means that the presented depths of the human organs during ultrasound imaging are not really accurate in those tissues that include other textures such as fat (Sprawls, 1993).

2.1.1.3 Wavelength of ultrasound wave

Wavelength of sound wave (λ) is a distance that the sound wave passes during the period of one oscillation. This parameter determines the length of the ultrasound pulse which affects ultrasound image resolution. The length characteristics of an ultrasound pulse are shown in Figure 2.2. Ultrasound pulse includes a number of wavelengths and the quantity of wavelengths throughout a pulse is defined with the damping characteristics of the transducer. The wavelength of the ultrasound beam is determined by the velocity (v) and frequency (f); as given by equation 2.5.

$$\lambda = \frac{v}{f} \quad (2.5)$$

The wavelength of an ultrasound wave is defined by transducer frequency and specification of the material which the ultrasound wave is travelling through. In order to have high resolution in ultrasound imaging, it is necessary to have a short pulse which is the result of short wavelength and high frequency. The relationship between the wave length and frequency is illustrated in Figure 2.3.

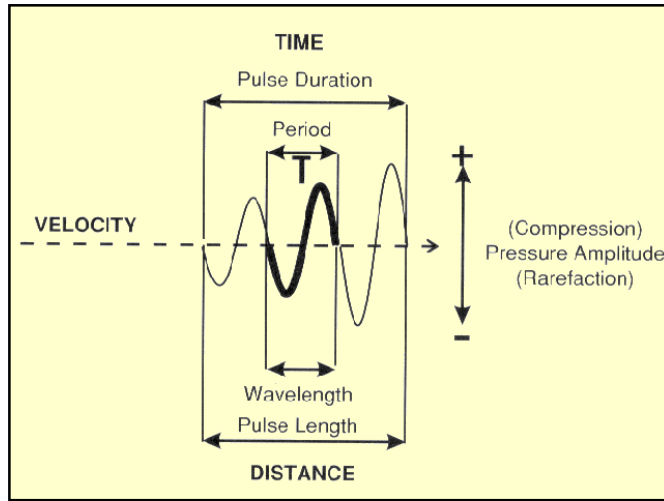


Figure 2.2. The length characteristics of an ultrasound pulse

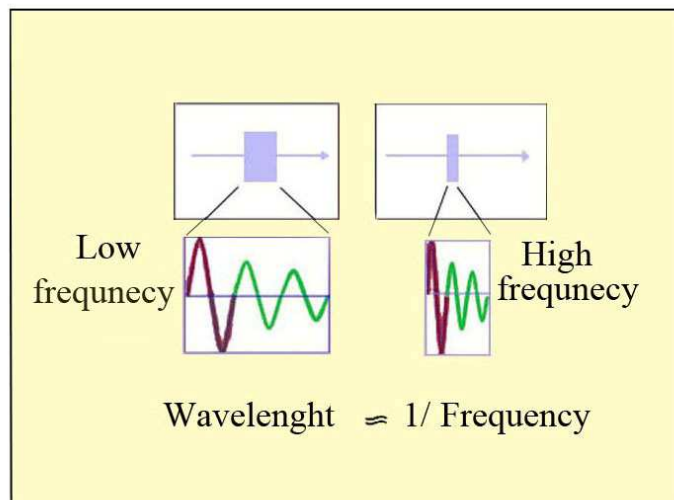


Figure 2.3. Dependency of ultrasound pulse length on wavelength and frequency.

2.1.1.4 Amplitude of ultrasound wave

The amplitude of an ultrasound pulse refers to the maximum pressure variation. The wave pressure is related to the value of tissue dislocation caused by the oscillation. In addition, the amplitude of an ultrasound beam shows the amount of energy of an ultrasound beam. The relationship between wave energy (E) and amplitude (A) is expressed in equation 2.6.

$$E \propto A^2 \quad (2.6)$$

In diagnostic ultrasound, it is essential to know the relative amplitude of ultrasound beams to recognize the reduction in the amplitude of an ultrasound pulse as it travels within a depth of the body structure. The relative amplitude of the ultrasound beam is expressed by equation 2.7.

$$\text{Relative Amplitude (dB)} = 20 \log (A/A_0) \quad (2.7)$$

where, A_0 is the initial amplitude.

2.1.2 Intensity of ultrasound wave

As an ultrasound pulse travels through a tissue, it transfers energy through the texture. The rate of transferred energy is called power and its unit is Watt. Power per unit of an area is expressed as intensity. In SI unit, the unit for the wave intensity is W/cm^2 . The relative intensity is expressed in equation 2.8 by the unit of decibel.

$$\text{Relative Intensity} = 10 \log (I/ I_0) \quad (2.8)$$

where, I_0 is the reference intensity.

2.1.3 Acoustical impedance

Acoustic impedance is the characteristic of the media which shows the resistance of tissue to the propagating of ultrasound wave. The higher acoustic mismatch the higher reflection and the lesser transmission. Acoustic impedance depends on the density (ρ) of tissue and speed of sound (v) and is expressed by equation 2.9. Acoustical impedance of some human tissues is presented in Table 2.2.

$$Z = \rho v \quad (2.9)$$

Table 2.2. Acoustic impedance of human tissues (Hendee and Ritenour, 2002).

Material	Acoustic Impedance (Kg.m⁻².s⁻¹)
Fat	1.38
Blood	1.61
Kidney	1.62
Soft tissue	1.63
Liver	1.65
Muscle	1.70
Lens of eye	1.85
Skull bone	6.10

The significances of acoustic impedance are as follows:

- a. Determining the acoustic transmission and reflection at the interfaces of two mediums with different acoustic impedances.
- b. Evaluating the absorption of ultrasound pulse in the material
- c. Designing ultrasound transducer (Hendee and Ritenour, 2002).

2.1.4 Interactions of ultrasound pulse with matter

As an ultrasound pulse penetrates through a medium like human tissues, it interacts in several ways. A number of these interactions are essential to obtain high resolution ultrasound image, and others are objectionable for ultrasound image and cause artifacts. Therefore, the capability to obtain and interpret ultrasonic images depends on accurate knowledge of the ultrasound pulse interactions.

2.1.4.1 Reflection of ultrasound pulse

As an ultrasound pulse reaches the tissue boundary, part of the pulse is reflected back to the transducer, and another part penetrates the organ. The amount of reflection depends on the difference of acoustic impedance of the two mediums, and it determines the brightness of the structure. Ultrasound imaging is based on the fact that, different organs have different densities and acoustical impedances, and this difference causes different reflections. The reflection is expressed in equation 2.10.

$$\text{Reflection (dB)} = 20 \log \frac{Z_2 - Z_1}{Z_2 + Z_1} \quad (2.10)$$

where, Z_1 and Z_2 represent the acoustic impedances of the two tissues on each side of the interface.

The reflection coefficient shows the relative amount of intensity of reflected wave to the incident wave and is expressed by equation 2.11.

$$R = \frac{Z_2 - Z_1}{Z_2 + Z_1} \quad (2.11)$$

The transmission coefficient shows the relative amount of intensity of transmitted wave across an interface to the incident wave and is given by equation 2.12.

$$T = \frac{4 Z_1 Z_2}{(Z_1 + Z_2)^2} \quad (2.12)$$

Since the amount of reflected wave plus the transmitted wave must be equal the total amount of incident wave, the transmission coefficient plus the reflection coefficient is equal one.

$$T + R = 1$$

High acoustic impedance mismatch at an interface, causes much of the energy of an ultrasound pulse be reflected, and only a small amount of ultrasound pulse be transmitted across the interface. For example, ultrasound pulse are reflected strongly at air–tissue and air–water interfaces because the acoustic impedance of air is much less

than that acoustic impedance of tissue or water. Reflection of ultrasound pulse, while it passes through tissue boundaries, is shown in Figure 2.4.

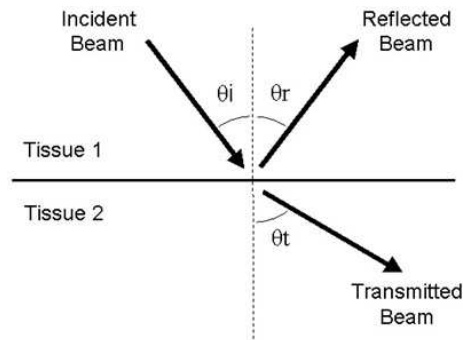


Figure 2.4. Reflected ultrasound beam from interface between two tissues. θ_i is the angle of incidence, θ_r is the angle of reflection and θ_t is the angle of transmission.

2.1.4.2 Refraction of ultrasound pulse

As an ultrasound pulse crosses tissue boundaries, due to the difference in the velocity of ultrasound in different mediums, the proportion of the ultrasound beam that is transmitted through the tissues undergoes refraction. This physical phenomenon causes some artifacts such as the double image artifact. Refraction can also be used for developing image quality by using acoustic lenses (Hendee and Ritenour, 2002; Sprawls, 1993). Refraction of ultrasound pulse while it passes through the tissue boundaries is illustrated in Figure 2.5.

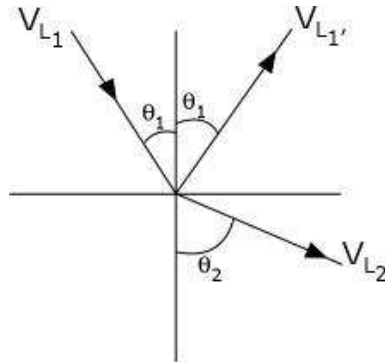


Figure 2.5. The passing ultrasound wave at the interface between two matters and produce refraction and bending. θ_1 is the angle of incidence and θ_2 is the angle of refraction.

Snell's law explains the relationship between the incident angle, reflection angle and the velocities of the wave while passes the tissue boundary and is given by equation 2.13.

$$\frac{\sin \theta_1}{V_{L1}} = \frac{\sin \theta_2}{V_{L2}} \quad (2.13)$$

where, V_{L1} and V_{L2} are the longitudinal wave velocities in materials 1 and 2, respectively. θ_1 is the angle of incidence and θ_2 is the angle of reflection.

2.1.4.3 Attenuation of ultrasound pulse

The term of attenuation refers to any mechanism that removes energy from the ultrasound pulse. As the ultrasound pulse passes through tissues its energy decreases leading to the formation of the ultrasound image. Attenuation can be as a result of absorption, reflection and scattering of the ultrasound pulse.

The major factor that causes attenuation is the conversion of the sound energy to the thermal energy. The significances of absorption are:

- a. Absorption limits the penetration's depth of the signal.
- b. The absorbed energy must be controlled because the tissues do not undergo unsafe heating (Hendee and Ritenour, 2002; Sprawls, 1993).

Absorption depends on the density of tissue and the frequency of the ultrasound beam. The greater the density and frequency cause greater absorption. Figure 2.6 shows a reduction in pulse amplitude as ultrasound travels through various tissues in the human body.

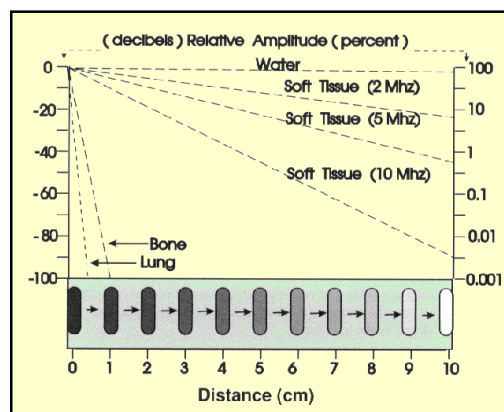


Figure 2.6. The effect of absorption on ultrasound pulse amplitude in relation to distance or depth in the body (Sprawls, 1993).

The value of attenuation changes directly with the frequency of the ultrasound pulse and the distance. The higher the frequency and distances, the more attenuation gained. In general, a high frequency ultrasound wave is associated with high attenuation, and it causes limitation for the penetration of ultrasound pulse, whereas a low frequency ultrasound wave is associated with low attenuation and deep tissue penetration.

Attenuation is evaluated in dBcm^{-1} of tissue and is represented by the attenuation coefficient. Attenuation is expressed by equation 2.14.

$$\text{Attenuation loss (dB)} = \alpha f x \quad (2.14)$$

where α is the attenuation coefficient (in dBcm^{-1} at 1 MHz), f is the ultrasound frequency, in MHz and x is the thickness of the material.

Most of the internal soft organs of the body have attenuation coefficient values of about $1\text{dBcm}^{-1}\text{MHz}^{-1}$, except for fat and muscle. In comparison to the soft tissues in the human's body, bone has a relatively high attenuation rate. (Hendee and Ritenour, 2002; Sprawls, 1993;). Ultrasound attenuation coefficient as a function of frequency for various tissue samples is shown in Figure 2.7.

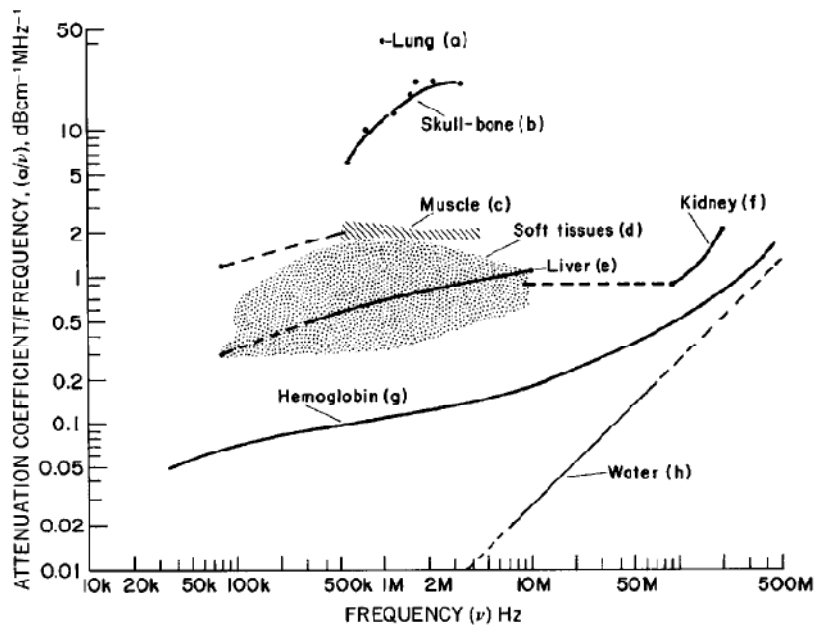


Figure 2.7. Ultrasound attenuation coefficient as a function of frequency for various tissue samples (Wells, 1975).

2.1.5 Acoustic properties measurement

Application of ultrasound in medical science caused the requirement of measuring acoustic properties of substance in ultrasonic frequencies (Zeqiri *et al.*, 2010). The most common technique which is used to measure the acoustic properties of the material is transmission substitution technique or insertion technique. This technique is a comparison measurement method which employs water as the reference to study the transmission of ultrasonic waves at frequencies above 1 MHz through a solid, semi-solid or liquid-like sample immersed in water (Surry *et al.*, 2004).

2.1.5.1 Sound speed measurement

The basic parameter to assess the ultrasound image is the velocity of ultrasound wave in media. Velocity of sound is also called sonic speed or sound speed (Surry *et al.*, 2004; Athanasiou *et al.*, 2010).

The sound speed is measured by transmitting a pulse from a single crystal ultrasound transducer, through a water bath, to be received by another single crystal transducer, which is aligned with the first one. In order to measure the sound speed, the transit time of ultrasound pulse for distilled water and then with sample immersed in distilled water is measured. By knowing the sound velocity in water (C_w) and the thickness of the sample (Δx), the sound speed can be calculated by using equation 2.15.

$$C_s = \left(\frac{1}{C_w} - \frac{\Delta t}{\Delta x} \right)^{-1} \quad (2.15)$$

where, C_W represents sound speed in water, Δx the thickness of sample and Δt is the measured time shift upon displacement of the water with the sample. It is assumed that the sound speed in distilled water at room temperature is 1482.3 ms^{-1} .

2.1.5.2 Attenuation measurement

In order to measure the acoustic attenuation, the amplitude of ultrasound pulse for distilled water and then with sample immersed in distilled water is measured. The attenuation can be calculated by using equation 2.16. The used attenuation coefficient for water is $2.5 \times 10^{-4} f^2$ (Park *et al.*, 1996, Markham *et al.*, 1951).

$$\alpha_s = \alpha_W - \frac{1}{\Delta x} [\ln A_S - \ln (A_W - 2 \ln (1 - R))] \quad (2.16)$$

where, α_W is the attenuation coefficient of water, A_W is the amplitude of the received ultrasound pulse from distilled water, A_S is the amplitude of the received ultrasound pulse from the immersed sample in the water, Δx is the thickness of the sample and R is the acoustical reflection coefficient at the water/sample interface.

2.1.6 Artifacts in ultrasound images

An artifact in an ultrasonic image is any structure, which does not exist in the scanned structure. Generally, the ultrasound imaging artifacts are caused by resolution, propagation pathway and attenuation of the ultrasound beams. In addition, lateral and axial resolution limitations are artifacts that may be reasoned for missing the details of

the image or in some cases two neighboring organs be imaged as one. Apparent resolution near the transducer (speckle) is not directly due to structure texture but may be as a result of boundary effects from the distribution of scatters in the organ (Kermkau and Taylor, 1986; Huang *et al.*, 2007; Hulsmans *et al.*, 1995)

2.1.6.1 Reverberation artifact in ultrasound images

When an echo reaches the transducer in an indirect path or reflected back from a strong reflector like metal or air, it bounces back to the body. As a result, the ultrasound beam is reflected more than one time that leads to the occurrence of the reverberation artifact. This process causes the echo to return to the transducer after the time that is assumed for the echo to travel and it causes misinterpretation of the echo. The reflection between transducer and body can occur many times and due to the attenuation, each reflected beam is weaker than the previous one (Huang *et al.*, 2007; Hulsmans *et al.*, 1995; Kirberger and Mmedvet, 1995). Reverberation artifact is shown in Figure 2.8.



Figure 2.8. Reverberation artifacts (white arrows) can be seen during needle (yellow arrows) advancement in the infraclavicular region (USRA, 2008).

2.1.6.2 Mirror image artifact in ultrasound images

It is assumed in the ultrasound imaging that sound wave travels in a straight line but scattering violates this assumption and mirror artifact is the result of this conflict. Mirror artifact is a kind of reverberation artifact which occurs at highly reflective air /fluid boundaries such as the diaphragm lung interface and descending aorta. The first image is displayed in the exact place while the second picture is observed on the other side of the reflector (Huang *et al.*, 2007; Hulsmans *et al.*, 1995; Kirberger and Mmedvet, 1995). Mirror image artifact is illustrated in Figure 2.9.

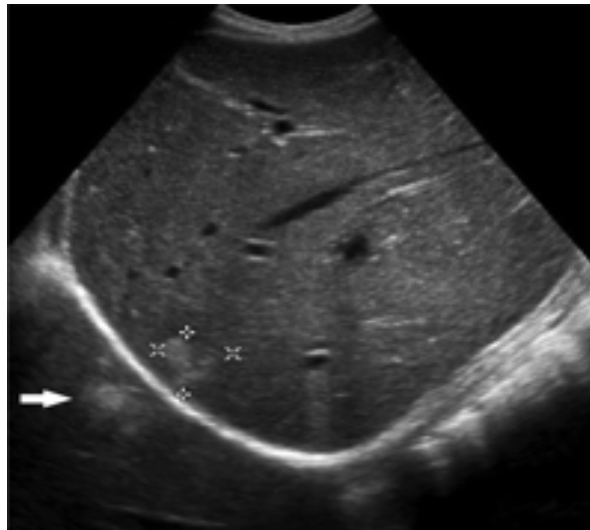


Figure 2.9. Longitudinal US image obtained at the level of the right hepatic lobe shows an echogenic lesion in the right hepatic lobe (cursors) and a duplicated echogenic lesion (arrow) equidistant from the diaphragm overlying the expected location of lung parenchyma (Feldman *et al.*, 2009).

2.1.6.3 Side lobe artifacts in ultrasound images

It is assumed in the ultrasound imaging that the lateral width of the ultrasound beam is extremely thin but diffraction violates this assumption and side lobe is the result of this conflict. While the main ultrasound beam is generating from transducer, side lobes and grating lobes are also producing and these lobes also have echoes which can be seen in the image. Side lobes artifact results from these echoes which is produced outside the main beam. This artifact can be generated from bowel gas adjacent to cystic structures (Huang *et al.*, 2007; Hulsmans *et al.*, 1995; Kirberger and Mmedvet, 1995). Side lobe artifact is shown in Figure 2.10.

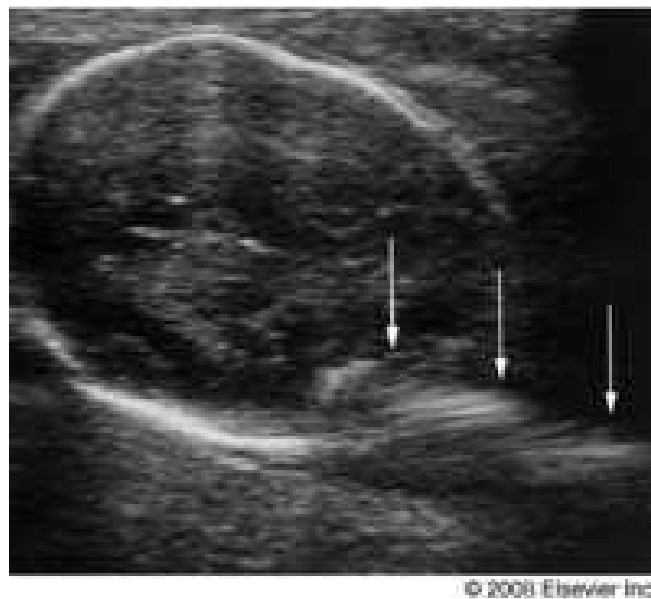


Figure 2.10. Side lobe artifact is seen overlying the fetal head (arrows). The artifactual nature of these echoes can be confirmed by noting that these echoes are not confined to the head but extend beyond its confines (Imaging consult, 2009).

2.1.6.4 Acoustic shadowing artifact in ultrasound images

When ultrasound pulse crosses through the tissue boundaries which have high absorption or high reflection, the most part of the pulse is attenuated. Thus the echo resulting from these phenomena is weak and it must travel to the transducer among the attenuating structures. So echoes from deeper organs are so weak and there is this possibility of not being detected. At the edge of gall bladder this kind of artifact may occur by small gallstone or at the edge of cyst or fetal body (Huang *et al.*, 2007; Hulsmans *et al.*, 1995; Kirberger and Mmedvet, 1995). Acoustic shadow artifact is illustrated in Figure 2.11.

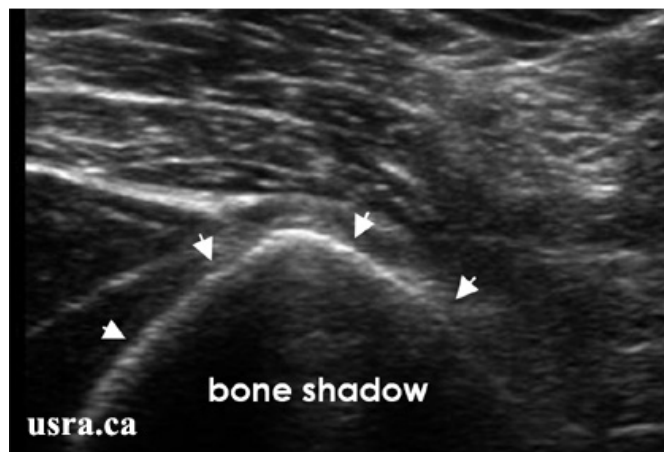


Figure 2.11. An acoustic shadow artifact (hypoechoic region = bone shadow) deep to a hyperechoic bone outline (arrows) is the result of beam attenuation when the beam encounters bone with a high attenuation coefficient (USRA, 2008).

2.2 Phantom